Proceedings IRF2018: 6th International Conference Integrity-Reliability-Failure
Lisbon/Portugal 22-26 July 2018. Editors J.F. Silva Gomes and S.A. Meguid
Publ. INEGI/FEUP (2018); ISBN: 978-989-20-8313-1

PAPER REF: 7284

INFLUENCE OF STIFFNESS AND STRENGTH DEGRADATION OF AN INFILL WALL UPON THE PERFORMANCE OF A TMD

Pedro L.P. Folhento[1(*)], Manuel T. Braz-César[2], António M.V. Paula[2], Rui C. Barros[3]
[1]Master in Civil Engineering, Polytechnic Institute of Bragança
[2]Department of Applied Mechanics, Polytechnic Institute of Bragança
[3]Department of Civil Engineering, Faculty of Engineering of the University of Porto
[(*)]*Email:* pedro.lp.folhento@gmail.com

ABSTRACT

The present work presents an investigation about the influence of an infill wall on the dynamic behavior of a tuned mass damper (TMD) designed to control lateral displacements of a framed building structure under seismic excitation. A Macro-Simulink model is used to simulate the hysteretic behavior of the infill wall under cyclic loading assuming two hysteretic models: stiffness degradation and strength degradation. A MATLAB/Simulink code was implemented to evaluate the influence of each model on the structural response of the controlled structure. Finally, the numerical results are presented and discussed for comparison and further studies.

Keywords: Structural control, passive systems, tuned mass dampers (TMD), hysteretic behavior.

INTRODUCTION

The use of vibration control systems in civil engineering applications, particularly passive control systems, has grown in recent years due to safety demands to protect critical facilities or buildings under natural hazard events such as strong winds or severe earthquakes. Given the reliability of passive systems, they are remarkably well accepted by engineers and constructors, and nowadays there are several civil structures equipped with base isolation, viscous dampers and tuned mass dampers (TMDs).

A common approach to design structural systems is to neglect the presence and therefore the behavior of non-structural components in the analysis. However, these elements can present a highly non-linear behavior with a large initial stiffness that can significantly influence the response of the structure. This approach should be evaluated whether such simplification is appropriate to design passive control systems for building structures. TMDs can be seen as secondary oscillators or harmonic absorbers designed to reduce the amplitude of structural or mechanical vibrations. The performance of these devices is strictly related with the accurate definition of the dynamic properties of the main structure. Thus, the existence of non-structural elements may influence the structural behavior, and consequently, the performance of the control system.

This paper is devoted to study the influence of an infill wall in the effectiveness of a TMD. A two degree-of-freedom (2-DOFs) system representing a single-story framed structure equipped with a TMD is used to assess the performance of the control system in the presence of the non-structural element. Stiffness and strength degradation models are used to represent the hysteretic response of the infill wall.

NUMERICAL MODEL

The numerical model of the controlled structure under the seismic excitation is shown in Figure 1. It shows a two degree-of-freedom (2-DOFs) system representing a single-story framed structure, m_1, equipped with a TMD, m_2. The main structure is connected to the exterior by a spring of stiffness k_1, and by a damping constant c_1. In the same way, the TMD is connected to the main structure by a spring of stiffness k_2, and by a damping constant c_2.

A Simulink model was implemented based on the properties of the structural system. It was considered in this study the following parameters: mass of the structure $m_1 = 5000kg$; the period $\mathrm{T} = 1.0\mathrm{s}$, the structural damping coefficient $\xi = 0.05$ and the mass ratio between the TMD and the structure $\mu = 0.15$.

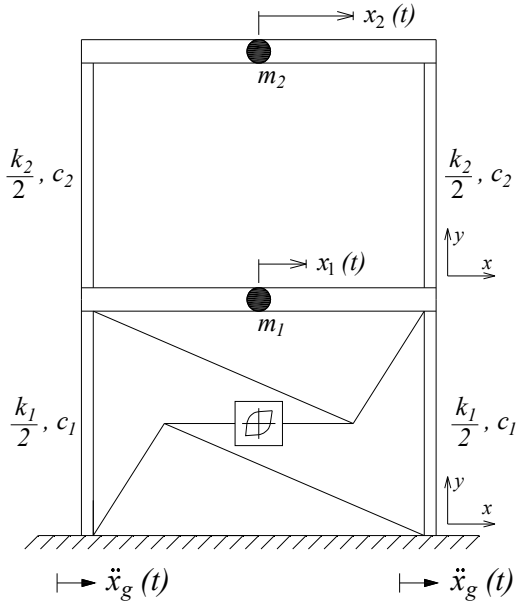

Fig. 1 - Schematic representation of the two DOFs structural system.

The Macro-Simulink numerical model is based on a smooth hysteretic model originally suggested by Bouc, 1967. The Macro-Simulink model used in this study was modified and adapted from Mousavi, *et al*, 2015 (Wen, 1976, Baber and Noori, 1985, Casciati, 1989, Reinhorn *et al.*, 1995, Oliveira, 1995, Sivaselvan and Reinhorn, 2000, Braz-César *et al*., 2013).

To verify the influence of an infill wall in the performance of a TMD, it was considered three cases of hysteretic behavior of the non-structural wall. The first case is a plain hysteretic behavior without any degradation. In the second case of hysteretic behavior only the stiffness degradation will be considered. The third case, in addition to the stiffness degradation, it will be considered the strength degradation of the non-structural wall.

Table 1 - Considered hysteretic parameters to simulate deferent frame behaviors (in all cases, $\boldsymbol{k_0 = 3\ \mathrm{MN/m}}$, $\boldsymbol{P_{fy} = 30\ \mathrm{kN}}$, $\boldsymbol{N = 5}$, $\boldsymbol{a = 0.03}$, $\boldsymbol{\eta = 1}$).

Case	Hysteretic behavior	α	β_1	β_2
0	Plain	50	0	0
I	Stiffness degradation	1	0	0
II	Stiffness and strength degradation	1	0.3	0.3

Mousavi, *et al.* 2015.

This study will be carried out using two different acceleration signals (Folhento, 2017). One represents a harmonic generic signal composed by five sections with different and growing acceleration as can be seen in Figure 2 and its corresponding function in Equation 1. The second proposed signal, represented in Figure 3, is the ground acceleration of the well-known El Centro earthquake, occurred in southeastern California on May 18, 1940.

$$\text{Generic Signal} \rightarrow \begin{cases} \sin(2\pi t), & \text{for} \quad 0s \le t < 4s \\ \frac{3}{2}\sin(2\pi t), & \text{for} \quad 4s \le t < 8s \\ 2\sin(2\pi t), & \text{for} \quad 8s \le t < 12s \\ 3\sin(2\pi t), & \text{for} \quad 12s \le t < 16s \\ 0, & \text{for} \quad t \ge 16s \end{cases} \tag{1}$$

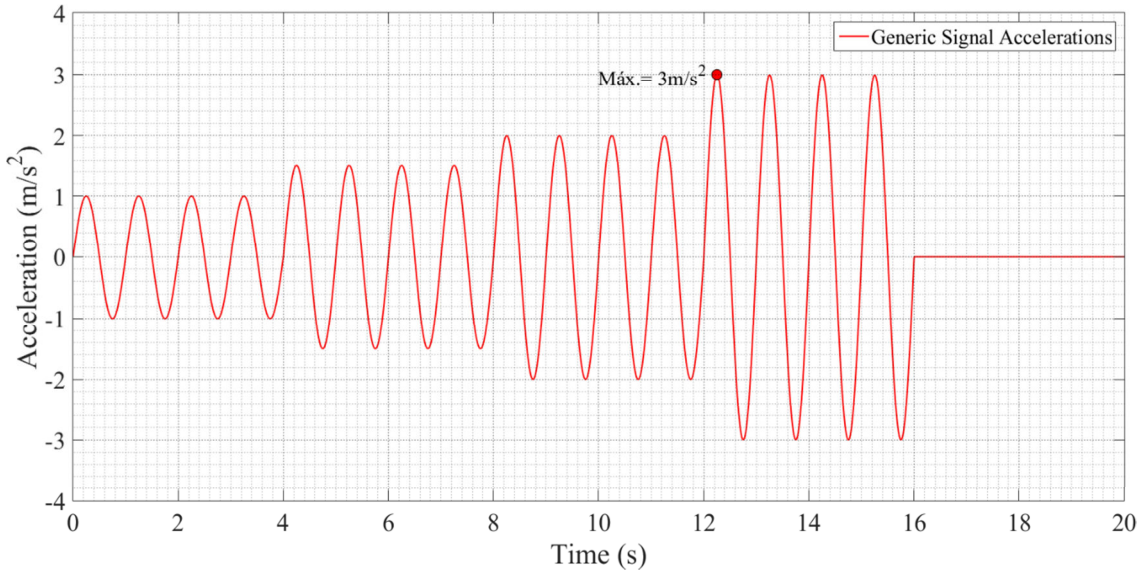

Fig. 2 - Generic harmonic signal accelerations.

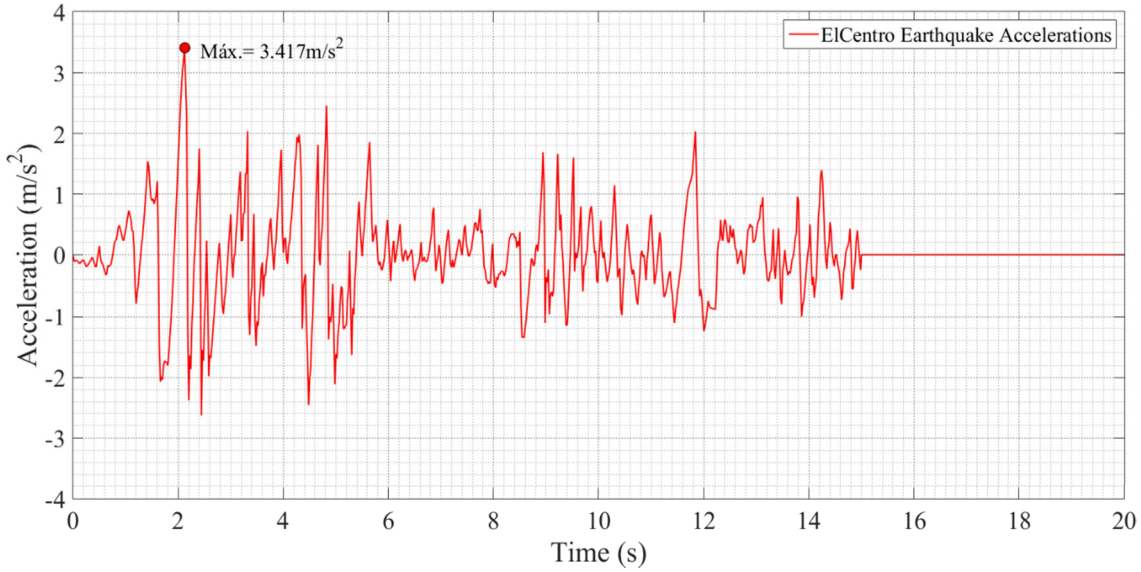

Fig. 3 - N-S component of El-Centro earthquake ground motion.

PLAIN HYSTERETIC BEHAVIOR (CASE 0)

A simple hysteretic behavior without degradation, suitable for well-detailed steel structures, e.g., special moment resisting frames (SMRFs), is represented by the following equations

$$P_f = k_f x = (a k_0 + k_{hyst}) x \tag{1}$$

$$k_{hyst} = (1-a) k_0 \left\{ 1 - \left| \frac{P_f}{P_{fy}} \right|^N \left[\eta \, sgn\left((1-a) P_f \dot{x} \right) + 1 - \eta \right] \right\} \tag{2}$$

where k_f is the nonlinear total lateral stiffness of the frame, k_0 is its initial lateral stiffness, a is the post-yield stiffness ratio, N a parameter that controls the transition smoothness from pre-yield to post-yield and η controls the shape of the discharge path. P_f and P_{fy} are the current frame shear and its yield value, respectively. Additionally, sgn is the signum function.

Using the previously mentioned numerical model, considering the case of plain hysteretic behavior of the frame (Case 0) and therefore using the Equations 2 and 3, based on the values of Table 1, the structural responses of the system represented in Figure 1, under the two accelerations considered in this study, one being the generic signal of growing acceleration and the other the seismic acceleration correspondent to the El Centro's earthquake, can be obtained.

The graph of Figure 4 shows the structural response of the structure under the generic signal acceleration, controlled or uncontrolled and with or without infill wall, in terms of displacements in respect to time.

In Figure 5 the graph displays the response in terms of displacements in respect to time of the second mass equivalent to the mass of the TMD, under the generic signal acceleration, being applied to the structure with or without infill wall.

The following two graphs describe the generalized force-displacement responses or hysteretic loops of the infill wall structure, under the generic acceleration, having on Figure 6(a) and (b) the uncontrolled and controlled response with the TMD with 15% of structure mass, respectively.

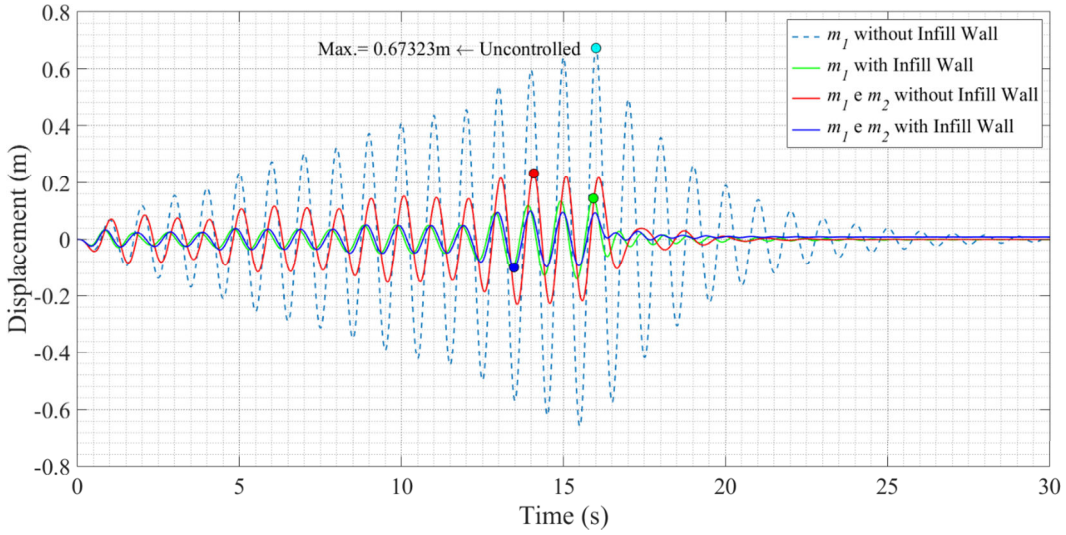

Fig. 4 - Displacement responses of the structure under the generic signal acceleration, considering Case 0 of hysteretic behavior.

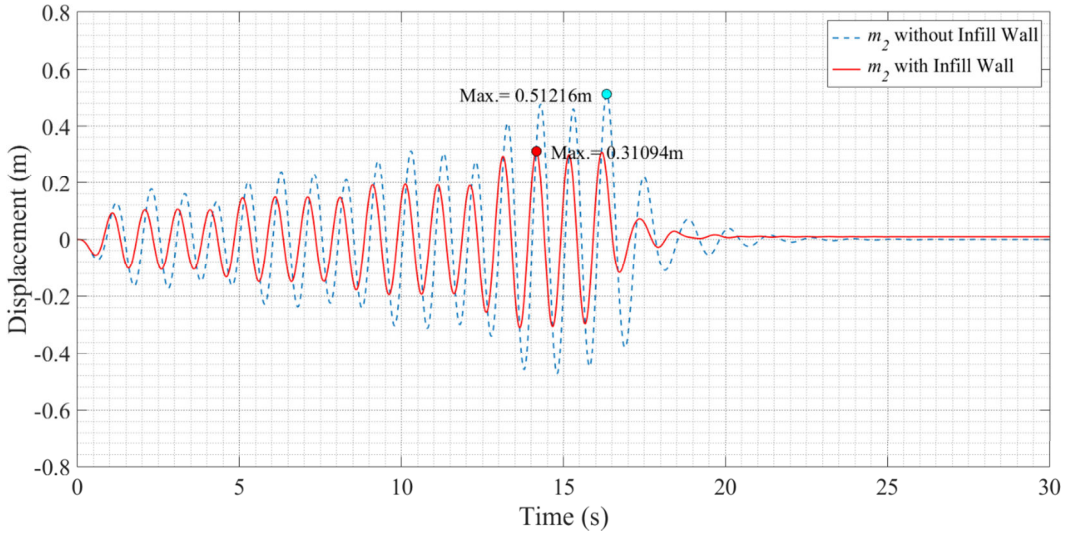

Fig. 5 - Displacement responses of the TMD under the generic signal acceleration, considering Case 0 of hysteretic behavior.

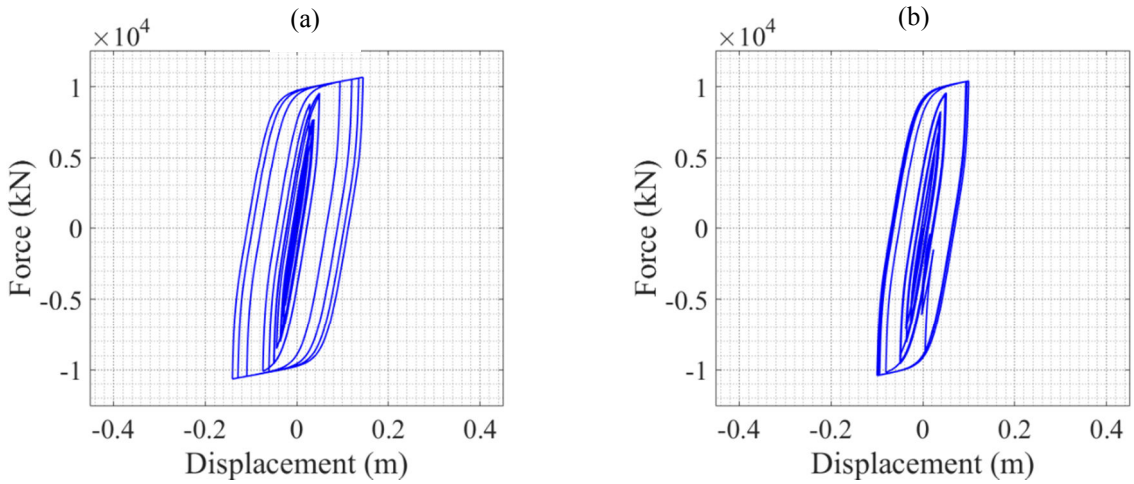

Fig. 6 - Hysteretic cycles of the infill wall structure under the generic signal acceleration, considering a plain hysteretic behavior (Case 0): (a) Uncontrolled response; (b) Controlled response with TMD.

Making use of the same numerical model, the structural responses of the system in study, subjected to the seismic acceleration of the El Centro's earthquake, can be found using the same expressions of the simple hysteretic behavior of the frame (Case 0).

Having this, Figure 7 therefore presents the response of the structure controlled or uncontrolled, with or without infill wall, in terms of displacements as a function of time.

Additionally, Figure 8 shows the response in terms of displacements in respect to time of only the passive control system, TMD, under the seismic acceleration, being applied to the structure with or without infill wall.

The graphs of Figure 9, display the hysteretic cycles, representing the relation between the force or strength capacity of the frame and its corresponding displacement, when subjected to the considered seismic acceleration. In which, Figure 9(a) shows the hysteretic loops of the uncontrolled system, opposing with the hysteretic loops of the controlled system with the TMD on Figure 9(b).

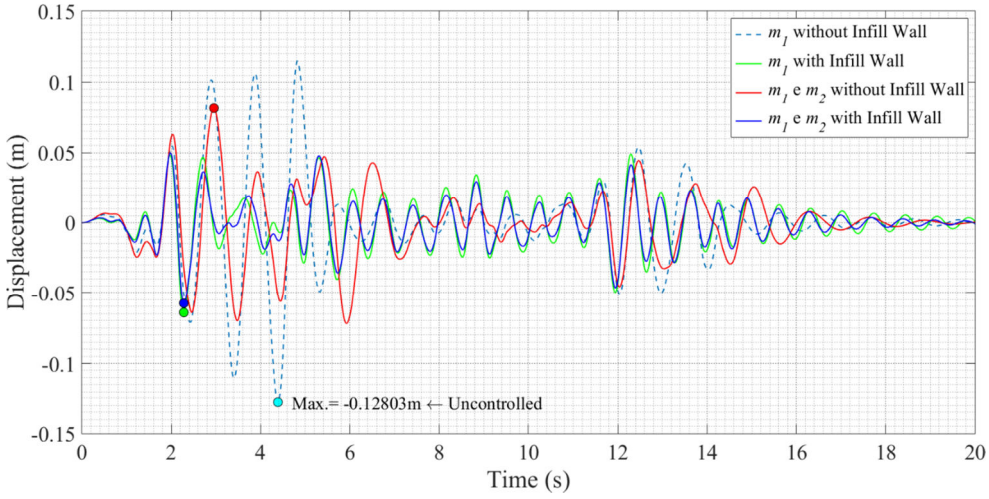

Fig. 7 - Displacement responses of the structure under the seismic acceleration, considering Case 0 of hysteretic behavior.

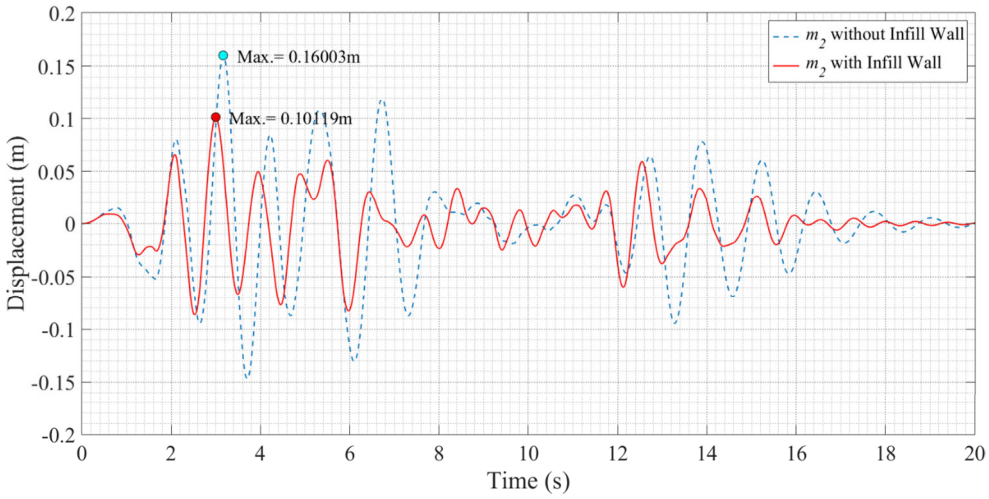

Fig. 8 - Displacement responses of the TMD under the seismic acceleration, considering Case 0 of hysteretic behavior.

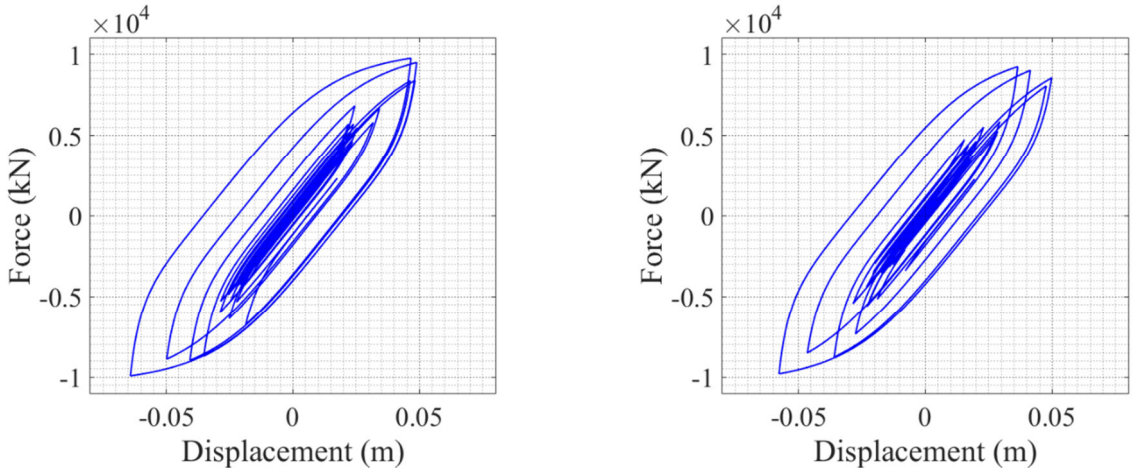

Fig. 9 - Hysteretic cycles of the infill wall structure under the seismic acceleration, considering a plain hysteretic behavior (Case 0): (a) Uncontrolled response; (b) Controlled response with TMD.

STIFFNESS DEGRADATION (CASE I)

The stiffness degradation arises from geometric effects. Elastic stiffness reduces with increased ductility. The stiffness degradation is implemented in the Macro-Simulink model through the so-called pivot rule (Park *et al.*, 1987). Most reinforced concrete undergoes stiffness degradation that should be accounted in a nonlinear dynamic analysis. To address this case, k_{hyst} should be modified as follows

$$k_{hyst} = (R_k - a)k_0\left\{1 - \left|\frac{P_f}{P_{fy}}\right|^N \left[\eta\,\mathrm{sgn}\left((1-a)P_f\dot{x}\right) + 1 - \eta\right]\right\} \tag{4}$$

where

$$P_f = k_f x = (ak_0 + k_{hyst})x \tag{5}$$

$$R_k = \frac{P_f + \alpha P_{fy}}{k_0 x + \alpha P_{fy}} \tag{6}$$

The parameter α can regulate the stiffness degradation. The higher the α, the lower the stiffness degradation. It should be pointed out that R_k in Equation 4 is a positive parameter and the unit is its maximum possible value. Nevertheless, R_k is also a decreasing function of time, since the stiffness of the structure would not increase after deterioration, regardless of the current displacement.

Considering now the stiffness degradation, using the Equations 4, 5 and 6, with the respective values presented in Table 1, the structural responses of the system illustrated in Figure 1, when subjected to the two considered accelerations signals in the present study, can be found by applying these considerations in the previously referred numerical model.

The structural responses are obtained in the same manner as the previous case of hysteretic behavior. Hence, the results relative to the system considering the stiffness degradation of the frame (Case I), under the generic signal acceleration are presented in Figures 10, 11 and 12. In like manner, the structural responses of the system admitting the same case of hysteretic behavior, under the seismic acceleration are shown in Figures 13, 14 and 15.

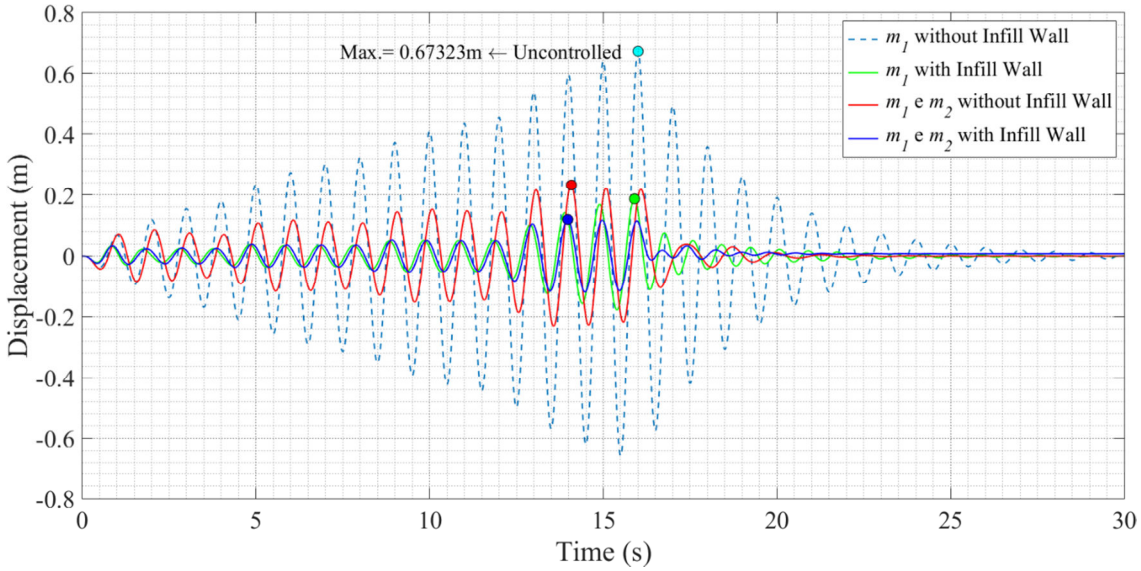

Fig. 10 - Displacement responses of the structure under the generic signal acceleration, considering Case I of hysteretic behavior.

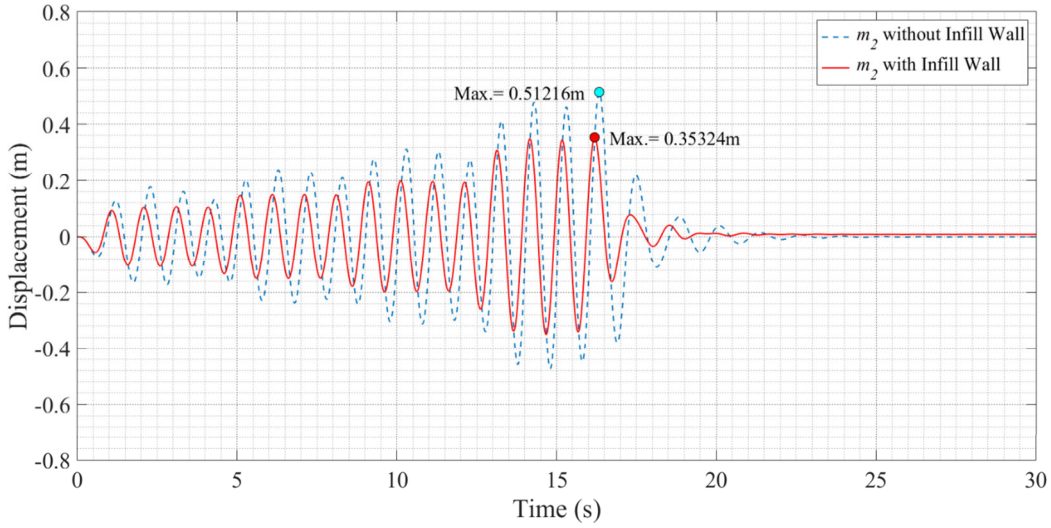

Fig. 11 - Displacement responses of the TMD under the generic signal acceleration, considering Case I of hysteretic behavior.

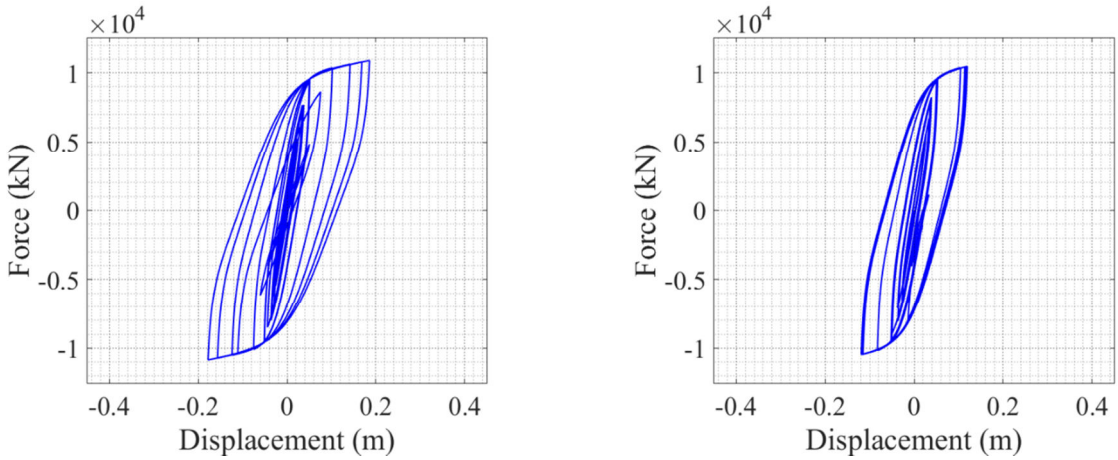

Fig. 12 - Hysteretic cycles of the infill wall structure under the generic signal acceleration, considering the stiffness degradation (Case I): (a) Uncontrolled response; (b) Controlled response with TMD.

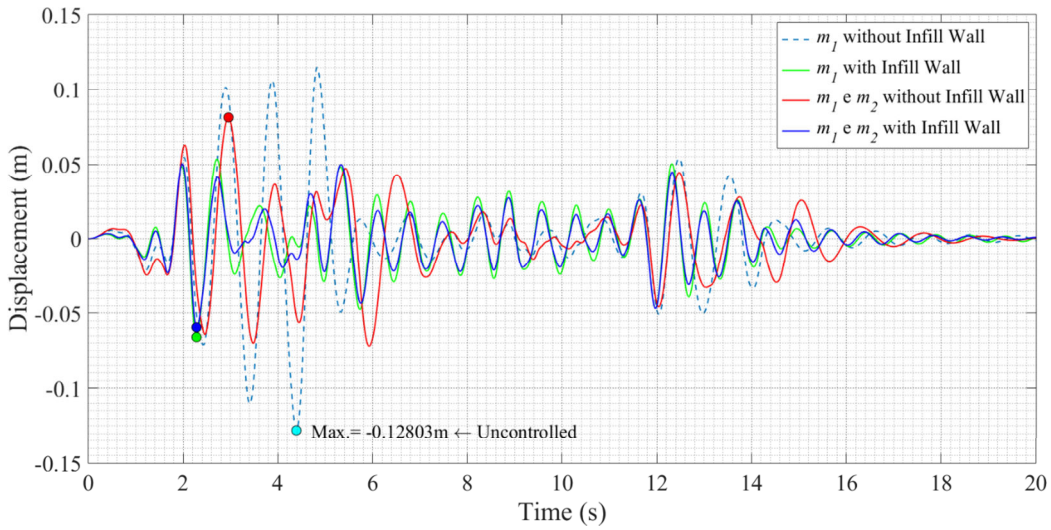

Fig. 13 - Displacement responses of the structure under the seismic acceleration, considering Case I of hysteretic behavior.

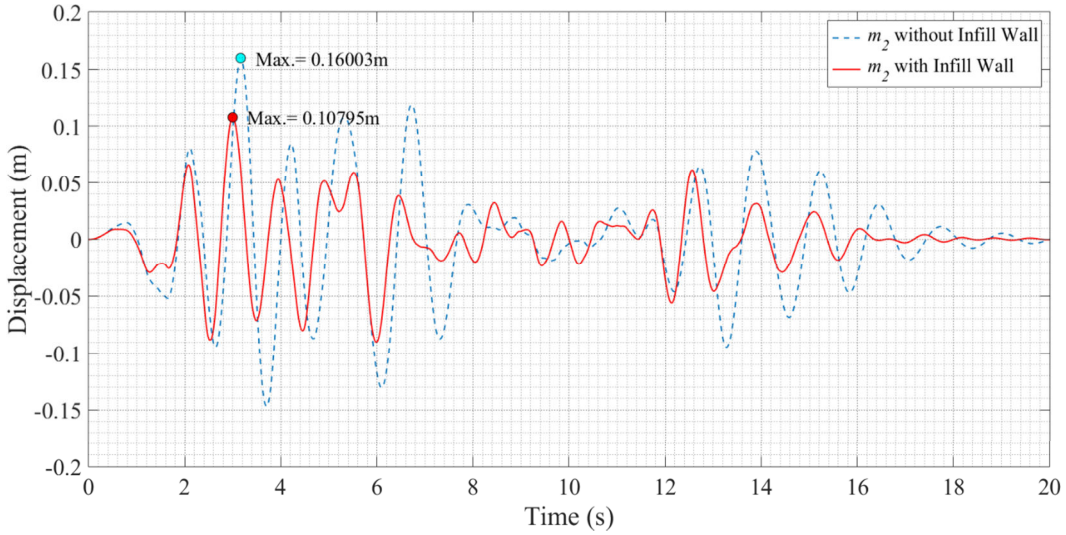

Fig. 14 - Displacement responses of the TMD under the seismic acceleration, considering Case I of hysteretic behavior.

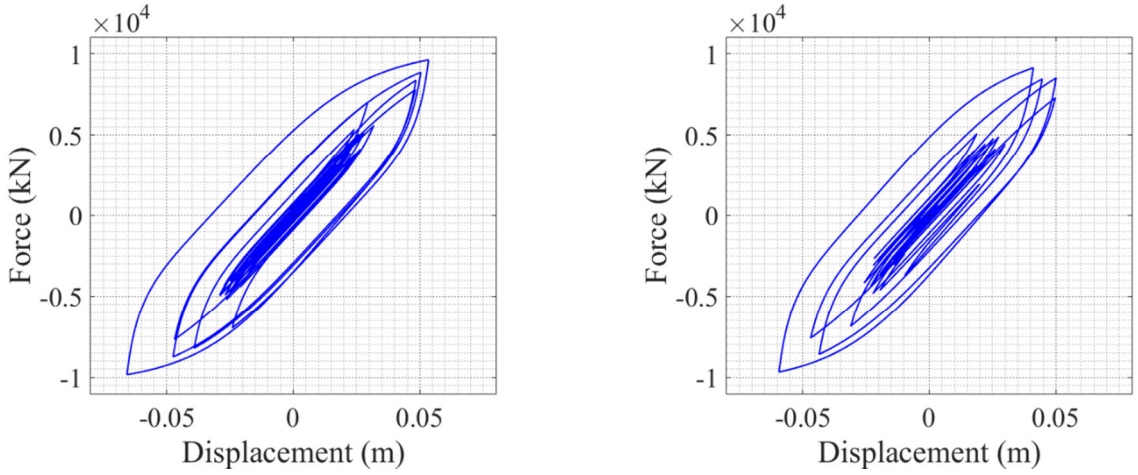

Fig. 15 - Hysteretic cycles of the infill wall structure under the seismic signal acceleration, considering the stiffness degradation (Case I): (a) Uncontrolled response; (b) Controlled response with TMD.

STIFFNESS AND STRENGTH DEGRADATION (CASE II)

To counteract the P-Δ effects, as well as the strength deterioration during repeated load inversions, a degradation of resistance based on energy/ductility is implemented in the Macro-Simulink model. This is achieved by the following modification on the yield strength.

$$P_{fy} = P_{fy0}\left[1-\left(\frac{x_{max}}{x_{ult}}\right)^{\frac{1}{\beta_1}}\right]\left[1-\frac{\beta_2 H}{(1-\beta_2)H_{ult}}\right] \tag{7}$$

The degraded and initial yielding strength of the frame are indicated by P_{fy} and P_{fy0}, respectively. The parameters $u_{\max}$ and u_{ult} are the maximum displacement in the current load inversion and the ultimate displacement capacity of the frame, respectively. The dissipated energy accumulated at the current displacement is represented by H and H_{ult} is the ultimate dissipated energy under monotonic (non-cyclic) load. Furthermore, β_1 and β_2 are degradation parameters based on ductility and energy dissipation demands, respectively.

Strength degradation should be considered for ordinary or intermediate moment resisting frames under great ductility demands. Most reinforced concrete frames and shear walls would also experience strength deterioration.

To consider the strength and stiffness degradation of the frame (Case II), the values presented in Table I corresponding to this case of hysteretic behavior must be applied in the Equation 7 and in the referred numerical model.

To obtain the structural responses considering the case with strength and stiffness degradation, the same procedure used in the previous simulations is carried out.

Thus, the results corresponding to the system subjected to the generic signal acceleration are presented in Figures 16, 17 and 18, as well as the results relative to the same system, but now under the seismic acceleration, are shown in Figures 19, 20 and 21.

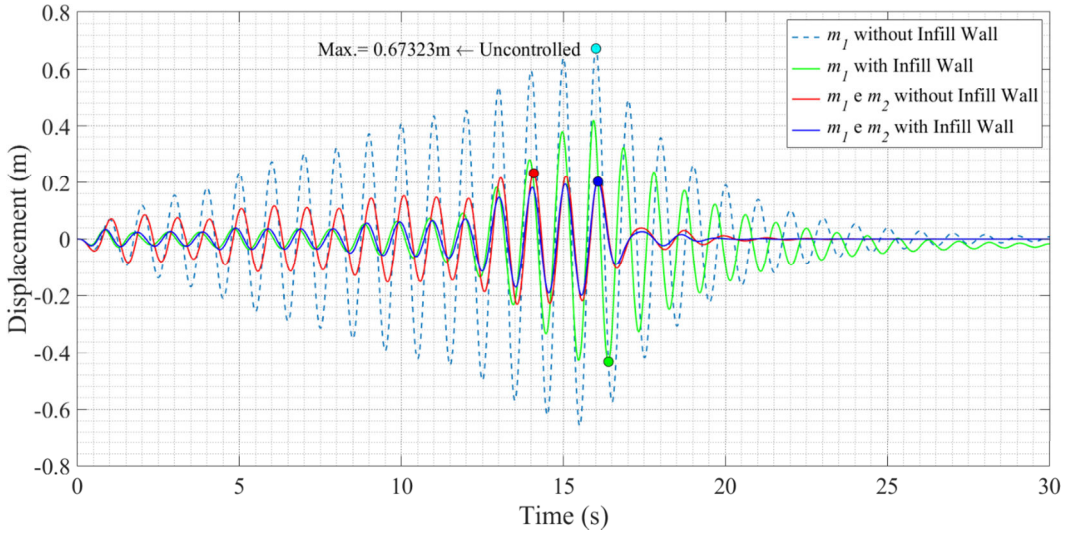

Fig. 16 - Displacement responses of the structure under the generic signal acceleration, considering Case II of hysteretic behavior.

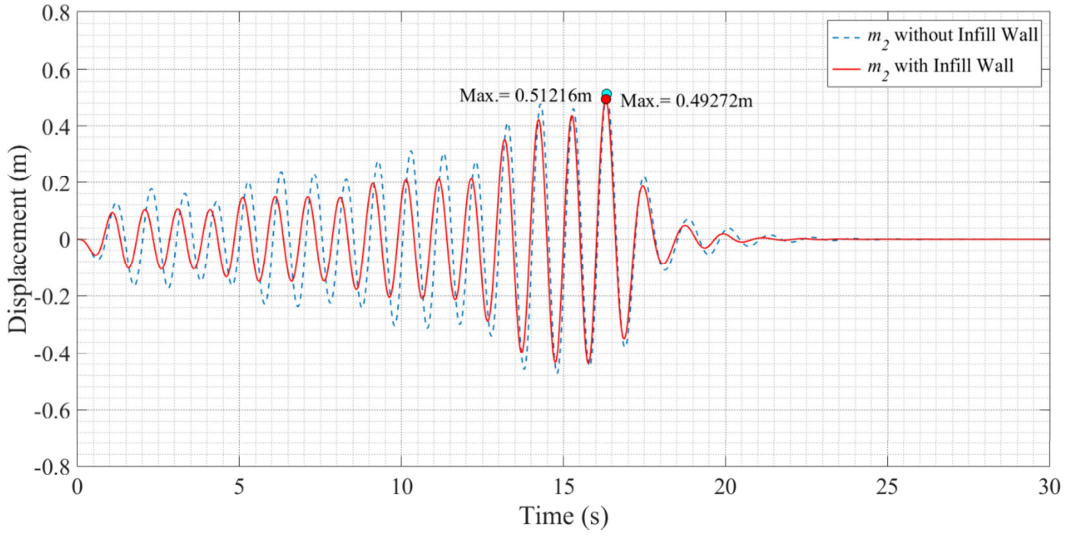

Fig. 17 - Displacement responses of the TMD under the generic signal acceleration, considering Case II of hysteretic behavior.

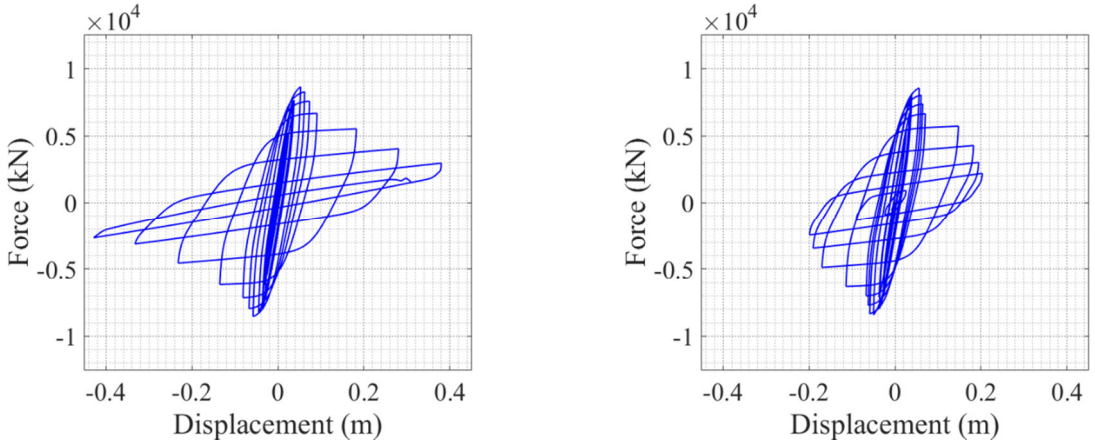

Fig. 18 - Hysteretic cycles of the infill wall structure under the generic signal acceleration, considering the stiffness and strength degradation (Case II): (a) Uncontrolled response; (b) Controlled response with TMD.

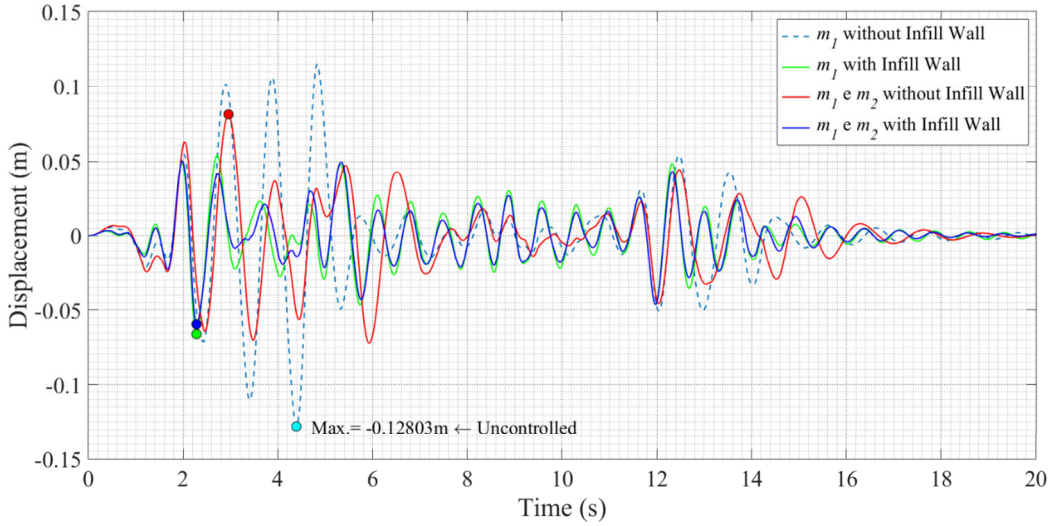

Fig. 19 - Displacement responses of the structure under the seismic acceleration, considering Case II of hysteretic behavior.

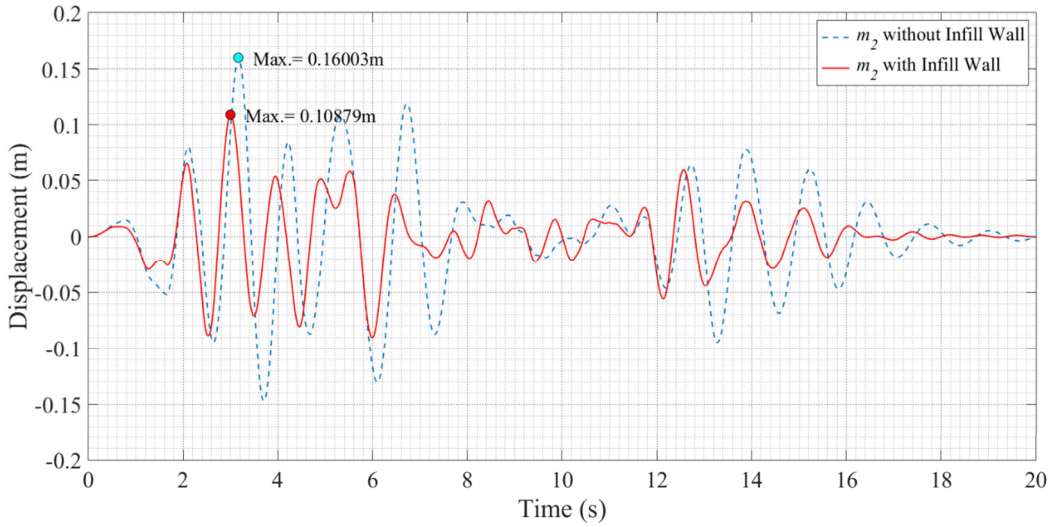

Fig. 20 - Displacement responses of the TMD under the seismic acceleration, considering Case II of hysteretic behavior.

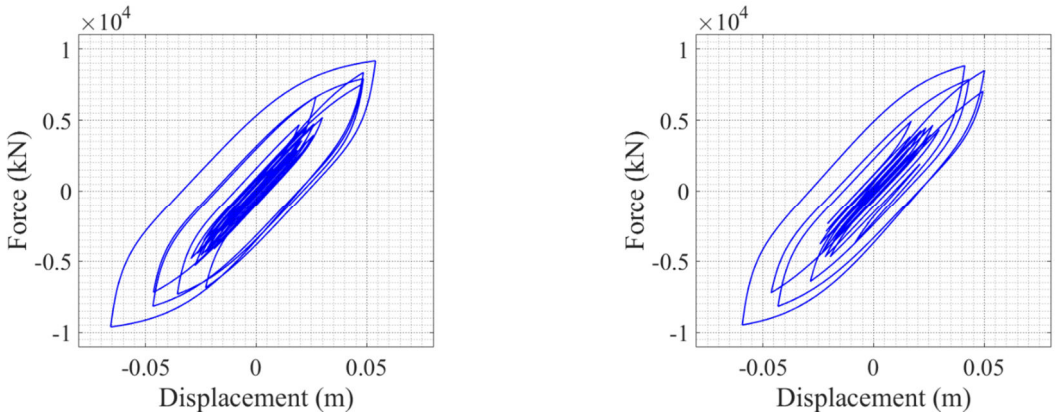

Fig. 21 - Hysteretic cycles of the infill wall structure under the seismic acceleration, considering the stiffness and strength degradation (Case II): (a) Uncontrolled response; (b) Controlled response with TMD.

RESULTS AND CONCLUSIONS

The results of the peak responses (considering displacements, velocities, accelerations and drift displacements between the structure and the TMD) of the system in study when requested by the generic signal and seismic accelerations, are presented in Table 2 and Table 3, respectively.

Based on the observation of Table 2, it can be always verified that the presence of a vibration control system, such as the TMD in this specific case, has an effective and positive influence on the structure in all cases and responses type, whenever it is filled or not with wall.

Analyzing now the different cases of hysteretic behavior of the frame, it can be seen that in a case where the stiffness and strength degradation are considered, the percentage of reduction with respect to the uncontrolled case is higher (in modulus) than other cases of hysteretic behavior. However, if the comparison was to be between the values of the infill wall structure controlled with the TMD, with the values of the uncontrolled structure without infill wall, it would be verified that the higher percentage of reduction would be seen in the case of simple hysteretic behavior.

Despite having a more irregular acceleration for the seismic signal, as natural from earthquakes, the same conclusions can be proved. Nonetheless, in the results with respect to the seismic request, the reductions are very small, verifying only slight reductions in between cases of hysteretic behavior, but on the other hand significant reductions in comparison with the uncontrolled case.

With the analysis of the peak responses, it can be concluded that as it moves on to a case of hysteretic behavior more realistic, i.e., plain hysteretic to strength and stiffness degradation, the reduction with respect to the uncontrolled structure without infill wall is smaller. Additionally, when the comparison is in between the cases of hysteretic behavior with respect to the corresponding case in the uncontrolled state, it can be concluded that in a case more realistic, the percentage of reduction is higher (in modulus). This can be verified on all responses types, i.e., displacements, velocities, accelerations and drift displacements.

Observing now in sequence the graphs of Figures 4, 10 and 16, it can be proved that the structural response of the infill wall structure, in terms of displacement, increases from the plain hysteretic behavior (Case 0) to the case where the stiffness and strength degradation (Case II) is considered (green and blue lines), corroborating with the prior paragraphs based on Table 2.

Table 2 - Peak responses of the structure under the generic signal acceleration.

Peak responses					
Case of hysteretic behavior		x (m)	$\dot{x}$ (m/s)	$\ddot{x}$ (m/s^2)	drift (m)
Uncontrolled	**Without infill wall**	0.673	4.184	26.565	0.673
	Case 0	0.145	0.860	6.357	0.145
	Case I	0.186	1.134	7.722	0.186
	Case II	0.433	2.929	24.342	0.433
Controlled with TMD	**Without infill wall**	0.233 (-189%) 0.512	1.443 (-190%) 2.947	9.007 (-195%) 18.267	0.233 (-189%) 0.484
	Case 0	0.100 (-45%) 0.311	0.604 (-42%) 1.918	4.406 (-44%) 11.997	0.100 (-45%) 0.285
	Case I	0.120 (-56%) 0.353	0.743 (-53%) 2.171	5.031 (-53%) 13.576	0.120 (-56%) 0.331
	Case II	0.203 (-113%) 0.493	1.252 (-134%) 2.725	7.908 (-208%) 16.796	0.192 (-126%) 0.378

a. The first and second lines represent the peak responses for the first and second floors, respectively, the main structure and the TMD.
b. The percentage on the left of the values stands for the percentage of increase or decrease of the peak responses with respect to the corresponding uncontrolled response.

Table 3 - Peak responses of the structure under the seismic acceleration of El Centro's earthquake.

Peak responses					
Case of hysteretic behavior		x (m)	$\dot{x}$ (m/s)	$\ddot{x}$ (m/s^2)	drift (m)
Uncontrolled	**Without infill wall**	0.128	0.906	7.025	0.128
	Case 0	0.064	0.627	6.391	0.064
	Case I	0.066	0.636	6.381	0.066
	Case II	0.066	0.635	6.353	0.066
Controlled with TMD	**Without infill wall**	0.081 (-57%) 0.160	0.577 (-57%) 0.922	4.854 (-45%) 5.899	0.081 (-57%) 0.147
	Case 0	0.058 (-11%) 0.101	0.610 (-3%) 0.643	6.007 (-6%) 5.206	0.058 (-11%) 0.106
	Case I	0.059 (-11%) 0.108	0.620 (-3%) 0.669	5.975 (-7%) 5.218	0.059 (-11%) 0.113
	Case II	0.059 (-11%) 0.109	0.619 (-3%) 0.669	5.952 (-7%) 5.196	0.059 (-11%) 0.113

a. The first and second lines represent the peak responses for the first and second floors, respectively, the main structure and the TMD.
b. The percentage on the left of the values stands for the percentage of increase or decrease of the peak responses with respect to the corresponding uncontrolled response.

In the same line of thought, seeing the graphs of Figures 7, 13 and 19 in sequence, which now consider that the system is subjected to the seismic acceleration instead of the generic signal acceleration, the changes between the different cases of hysteretic behavior are not very perceptive, since a seismic acceleration is very irregular, leading to a structural response also irregular. Although the structural response is irregular, the peak responses have a slight increase from the Case 0 to the Case II.

The same conclusions can be verified when observing sequentially the graphs of Figures 5, 11 and 17, in which the response of the TMD in terms of displacement increase from the Case 0 to the Case II, verifying that in the case of stiffness and strength degradation the response with infill wall has the smaller reduction in relation with the case without infill wall, when comparing it with the other cases of hysteretic behavior. The successively observation of the graphs of Figures 8, 14 and 20, considering now the seismic acceleration, leads to identical conclusions, although it has a slight increase in the displacement response from Case 0 to Case II it is not very perceptive.

Observing now the graphs of Figures 6, 12 and 18, showing the hysteretic loops of Cases 0, I and II, respectively, and focusing only on the uncontrolled cases, it can be seen that in the first case where stiffness degradation is not considered, the charge and discharge curves remain approximately parallels, meaning that the stiffness degradation is almost inexistence, since the stiffness is reflected by the slope of the charge and discharge curves. In addition, the fact that the system has great stiffness, leads to bigger displacements for higher values of the strength capacity of the frame. The evolution of the hysteretic cycles with the requested acceleration through time, implies a greater energy dissipation reflected by the increasing area of the cycles.

The stiffness degradation is now evident when observing the Figure 12 in particular, where now the slope of the charge and discharge curves vary from cycle to cycle. Also, the cycles area is less than the previous case, and it shows a slight increase of the displacement, for the same value of the strength capacity of the frame, when comparing it with the case of plain hysteretic behavior.

In the graphs of Figure 18 that show the case of stiffness and strength degradation, it can be observed that besides the slope variation of the charge and discharge curves, reflecting the stiffness degradation, a decreasing in strength capacity of the frame can also be verified, resulting in higher values of displacements. This is easily noted, since the transformation of the hysteretic cycles form goes from vertical to horizontal form. This shows that in the earlier cycles of the uncontrolled case, the wall has strength capacity of approximately *900kN*, presenting displacements of about *5cm*, and in the last cycles has approximately *250kN*, for displacements of about *40cm*.

It should be noted that in the case that the strength degradation is added, the initial strength capacity is less than the previous case, in about *250kN*.

This situation resulted in a numerical instability, being necessary to interrupt purposely the numerical simulation at approximately *15.8s*. In reality, this translates into a structural instability of the wall, more specifically the failure of the wall out of its plane. This fact can be easily proved by the observation of the graph of Figure 16, where the “green line” presents a permanent displacement of about *5cm* comparing it with its original position.

The same characteristics of the hysteretic loops may be withdrawn when observing the controlled cases. However, the presence of the vibration control system, in this case the TMD, shows a significant reduction of the displacements preserving the same strength capacity of the wall. The presence of the TMD also provides a less contribution of the wall in the action of energy dissipation.

Also, it should be pointed out that the structural instability no longer happens in the presence of the TMD, which can be seen in the graph of Figure 16 (blue line) and on the graph of Figure 18(b).

By the observation of Figures 9, 15 and 21, in which the seismic acceleration is now considered, despite the irregularity of the hysteretic cycles, the same conclusions and characteristics can be applied, despite not being so obvious. Nevertheless, the presence of the TMD still reduces significantly the displacements of the wall, providing less contribution of the wall in the energy dissipation.

REFERENCES

[1] Baber, T. T., and Noori, M. N. (1985). Article. Random Vibration of Degrading, Pinching Systems. J. Engrg. Mech., ASCE, 111(8), pp. 1010-1026.

[2] Casciati, F. (1989). Article. Stochastic Dynamics of Hysteretic Media. Amsterdam: Struct. Safety, 6, pp. 259-269.

[3] Bouc, R. (1967). Article. Forced Vibration of Mechanical Systems with Hysteresis. Proceedings 4th Conf. on Non-linear Oscillations.

[4] Braz-César M., Oliveira D., Barros R. (2013) Validação Numérica da Resposta Cíclica Experimental de Pórticos de Betão Armado (in portuguese). Revista da Associação Portuguesa de Análise Experimental de Tensões - Mecânica Experimental, 22, pp. 1-13.

[5] Folhento P., (2017) Estudo da Influência de Paredes de Alvenaria no Desempenho de Amortecedores de Massa Sintonizada. MSc Thesis, Politechnic Institute of Bragança.

[6] Mousavi, S. A., Zahrai, M. S., and Saatcioglu, M. (2015). Article. Toward Buckling Free Tension-Only Braces Using Slack Free Connections. Journal of Constructional Steel Reasearch, Vol. 115, pp. 329-345 - ELSEVIER.

[7] Oliveira D., (1995) Comportamento de Pórticos de Betão Armado Preenchidos com Paredes de Alvenaria (in portuguese). MSc thesis, University of Porto.

[8] Park, Y. J., Ang, A. H.-S., and Wen, Y. K. (1987). Article. Damage - Limiting Aseismic Design of Buildings. Earthquake Spectra, Vol. 3, Nº1.

[9] Reinhorn, A. M., Madan, A., Valles, R. E., Reinchmann, Y., and Mander, J. B. (1995). Technical Report NCEER-95-0018. Modeling of Masonry Infill Panels for Structural Analysis. State University of New York at Buffalo, Buffalo, N.Y.

[10] Sivaselvan, M. (2013) Hysteretic models with stiffness and strength degradation in a mathematical programming format, International Journal of Non-Linear Mechanics, 51, pp. 10-27.

[11] Sivaselvan, M. V., and Reinhorn, A. M. (2000). Article. Hysteretic Models for Deteriorating Ineslatic Structures. Journal of Engineering Mechanics, Vol. 126, Issue 6, pp. 633-640.

[12] Wen, Y.-K. (1976). Article. Method for Random Vibration of Vibration of Hysteretic Systems. J. Engrg. Mech. Div., ASCE, 102(2), pp. 249-263.